DOI:
10.1016/j.hrthm.2020.03.021

Document Version
Version created as part of publication process; publisher's layout; not normally made publicly available

Journal Pre-proof

Left ventricular endocardial pacing is less arrhythmogenic than conventional epicardial pacing when pacing in proximity to scar

Caroline Mendonca Costa, PhD, Aurel Neic, PhD, Karli Gillette, MSc, Bradley Porter, MBBS, Justin Gould, MBBS, Baldeep Sidhu, MBBS, Zhong Chen, MBBS, Mark Elliott, MBBS, Vishal Mehta, MBBS, Gernot Plank, PhD, Christopher A. Rinaldi, MBBS, MD, FHRS, Martin J. Bishop, PhD, Steven A. Niederer, PhD

PII: S1547-5271(20)30282-4

DOI: https://doi.org/10.1016/j.hrthm.2020.03.021

Reference: HRTHM 8329

To appear in: *Heart Rhythm*

Received Date: 20 December 2019

Accepted Date: 21 March 2020

Please cite this article as: Costa CM, Neic A, Gillette K, Porter B, Gould J, Sidhu B, Chen Z, Elliott M, Mehta V, Plank G, Rinaldi CA, Bishop MJ, Niederer SA, Left ventricular endocardial pacing is less arrhythmogenic than conventional epicardial pacing when pacing in proximity to scar, *Heart Rhythm* (2020), doi: https://doi.org/10.1016/j.hrthm.2020.03.021.

Title: Left ventricular endocardial pacing is less arrhythmogenic than conventional epicardial pacing when pacing in proximity to scar

Short title: Arrhythmogenic risk during endocardial pacing

Caroline Mendonca Costa, PhD, King's College London, UK
Aurel Neic, PhD, Medical University of Graz, Austria
Karli Gillette, MSc, Medical University of Graz, Austria
Bradley Porter, MBBS, King's College London, UK
Justin Gould, MBBS, King's College London, UK
Baldeep Sidhu, MBBS, King's College London, UK
Zhong Chen, MBBS, King's College London, UK
Mark Elliott, MBBS, King's College London, UK
Vishal Mehta, MBBS, King's College London, UK
Gernot Plank, PhD, Medical University of Graz, Austria
Christopher A. Rinaldi, MBBS, MD, FHRS, Guy's and St. Thomas' Hospital, London, UK & King's College London, UK
Martin J. Bishop, PhD, King's College London, UK
Steven A. Niederer, PhD, King's College London, UK

Correspondence:
Dr. Caroline Mendonca Costa
The Rayne Institute, 4th Floor, Lambeth Wing
St Thomas' Hospital, London SE1 7EH
caroline.mendonca_costa@kcl.ac.uk

Conflicts of interest: None.

Word count: 4988

1. Abstract

Background: Epicardial pacing increases risk of ventricular tachycardia (VT) in patients with ischemic cardiomyopathy (ICM) when pacing in proximity to scar. Endocardial pacing may be less arrhythmogenic as it preserves the physiological sequence of activation and repolarization.

Objective: To determine the relative arrhythmogenic risk of endocardial compared to epicardial pacing, and the role of the transmural gradient of action potential duration (APD) and pacing location relative to scar on arrhythmogenic risk during endocardial pacing.

Methods: Computational models of ICM patients (n=24) were used to simulate left-ventricular (LV) epicardial and endocardial pacing at 0.2-3.5cm from a scar. Mechanisms were investigated in idealised models of the ventricular wall and scar. Simulations were run with/without a 20ms transmural APD gradient in the physiological direction and with the gradient inverted. Dispersion of repolarization was computed as a surrogate of VT risk.

Results: Patient-specific models with a physiological APD gradient predict that endocardial pacing decreases (34%, $P<0.05$) VT risk compared to epicardial pacing when pacing in proximity to scar (0.2cm). Endocardial pacing location does not significantly affect VT risk, but epicardial pacing at 0.2cm compared to 3.5cm from scar increases ($P<0.05$) it. Inverting the transmural APD gradient reverses this trend. Idealised models predict that propagation in the direction opposite to APD gradient decreases VT risk.

Conclusion: Endocardial pacing is less arrhythmogenic than epicardial pacing when pacing proximal to scar and is less susceptible to pacing location relative to scar. The physiological repolarization sequence during endocardial pacing mechanistically explains reduced VT risk compared to epicardial pacing.

Key words: Cardiac resynchronization therapy; ventricular tachycardia; infarct scar; patient-specific modelling; dispersion of repolarization

2. Introduction

Endocardial pacing has been shown to improve response to cardiac resynchronization therapy (CRT) in comparison to conventional LV epicardial pacing[1,2] due to access to fast endocardial conduction[3]. Epicardial pacing reverses the physiological sequence of activation and repolarization, which is known to increase dispersion of repolarization and facilitate arrhythmias[4]. Endocardial pacing may be less arrhythmogenic than epicardial pacing, as it preserves the physiological sequence of activation and repolarization.

Our previous study[5] predicted that conventional epicardial LV pacing in proximity to scar increases repolarisation gradients, that in turn increases VT risk by increasing the vulnerable window for uni-directional block. Endocardial pacing increases the area accessible for lead implantation, as it is not constrained by coronary sinus anatomy, allowing operators to target lead position based on the individual's anatomy and scar[6,7]. This enables pacing at an optimal location to maximize response while avoiding increasing VT risk. However, susceptibility to arrhythmogenesis during endocardial pacing has not been systematically investigated and the role of pacing location relative to scar during endocardial pacing is currently unknown.

The primary aim of this study is to investigate the relative arrhythmogenic risk of endocardial pacing compared with epicardial pacing. We also investigate the role of pacing location relative to scar during endocardial pacing, as done previously for epicardial pacing[5] and the role of the direction of transmural propagation during endocardial and epicardial pacing on VT risk. We use a virtual cohort of patient-specific computational models of LV anatomy, scar, and border zone (BZ) to run electrophysiology (EP) simulations and compute dispersion of repolarization as a surrogate for VT risk[5].

3. Methods

3.1. Models of patient-specific anatomy

We used 24 image-based patient-specific models of LV anatomy and scar morphology, as described previously[5]. Briefly, LV endocardium and epicardium contours were manually drawn in each short-axis slice of late gadolinium enhanced (LGE) MRI. Scar and BZ were segmented and reconstructed in 3D. A finite element tetrahedral mesh (mean edge length of 0.8mm) was generated and 3D reconstructed

scar and BZ segmentations[8] were mapped onto it. Rule-based fibres were assigned to the models[9]. An example is shown in Figure 1A. These models are available online (http://doi.org/doi:10.18742/RDM01-570).

3.2. Idealised models

We created idealised models of a ventricular wall wedge to investigate the role of transmural APD gradient direction relative to pacing location (endocardium or epicardium) independently of the effects of ventricle anatomy. A 10x10x1cm^3 mesh of tetrahedral elements was created, with mean edge length of 800um. LV fibre orientations were assigned using a rule-based method[9]. A circumferential and transmural scar with radius of 1.5cm and a 0.2cm thick BZ were included on the left side of the mesh (Figure 1B).

3.3. Selecting pacing locations

Pacing locations were selected on the endocardial and epicardial LV surfaces transmurally-opposite to each other. For the patient-specific models, pacing locations were selected at 0.2, 0.5, 1.5, 2.5, and 3.5cm from scar (Figure 1A), and at 0.2 and 3.5cm (Figure 1B) for the idealised model. Distances from scar were computed using Eikonal simulations[5].

3.4. Fast endocardial conduction layer

The presence of fast endocardial conduction (FEC) is thought to improve response to endocardial CRT[3]. Using the transmural coordinate of the universal ventricular coordinates system[10], we selected a 1mm thick FEC layer[3] in each anatomical model. This layer was selected within the entire endocardial surface including healthy, BZ and scar tissue (Figure 2A).

3.5. Electrophysiology models and parameters

Activation and repolarization sequences were simulated, as in our previous study[5]. Briefly, the Reaction-Eikonal model[11] coupled to the ten Tusscher[12] model of human ventricular action potential were used and activation was initiated at each pacing location. Transversely isotropic conduction velocities (CV) of 0.67 and 0.3m/s[13] were prescribed to healthy tissue in the longitudinal and transverse directions,

respectively. An isotropic CV of 0.15m/s was prescribed to the BZ[14] and the scar core was modelled as non-conducting.

To the best of our knowledge, no CV measurements within a FEC layer in the presence of an infarct scar are currently available in the literature. Based on CV measurements within a FEC layer[15] and BZ[14], we created 6 different FEC setups, where a 2x faster CV was prescribed to the FEC layer over healthy tissue along the fibre direction[15] and an isotropic CV either 2x faster than healthy or BZ tissue was prescribed to the FEC layer over BZ/scar. The individual setups are detailed in Supplemental Table S1. Unless otherwise stated, we show results with a FEC layer over healthy and BZ tissue, with a 2x faster CV over healthy tissue along the fibre direction and an isotropic CV 2x faster than BZ tissue (Setup 4 in Supplemental Table S1).

To investigate the role of transmural APD heterogeneity on arrhythmogenesis, a linear change in transmural APD of 20ms was implemented across the ventricular wall in line with previous measurements of transmural APD heterogeneity in heart failure (HF)[16]. This was achieved by multiplying the conductance of the slow rectifying potassium current, gKs, by a factor of 0.7 to 1 giving an APD of 280 to 260ms, respectively, and reflecting a 20ms APD gradient[16]. An inverted gradient was also implemented. An example of the transmural APD gradients is shown in Figure 2B.

We present results with the patient-specific models for a control model (20ms APD gradient in the physiological direction), a model with no APD gradient, and a model with an inverted APD gradient (opposite to physiological direction). All model results presented in the main article include a FEC layer as in Setup 4 of Supplemental Table S1. Results with different FEC setups are shown in the Supplement.

3.6. Computing dispersion of repolarization

We used the volume of high repolarization gradients (HRG) within 1 cm around the scar as a metric of local dispersion of repolarization and a surrogate for arrhythmogenic risk, as done previously[5]. Briefly, repolarization times, local repolarization gradients, and the volume of tissue with repolarization gradients above a threshold of 3ms/mm[17] were computed.

3.7. Statistical analysis

Balanced one-way ANOVA with Tukey-Kramer post-hoc tests were used to compare the HRG volume between the patient-specific pacing locations. Paired t-tests (Student's test) were used to compare the HRG volume between endocardial and epicardial pacing at each pacing location. Quantitative results are shown as standard bar plots including error bars, which describe the standard variation of values within the 24 patient models. A P-value smaller than 0.05 was considered significant.

4. Results

4.1. Pacing location and modality

We computed repolarization gradients and the HRG volume using our control model. Figure 3C shows a significant reduction in the HRG volume when pacing away from the scar for epicardial (black) but not for endocardial (red) pacing. Specifically, the HRG volume is significantly smaller when pacing at 3.5cm than 0.2cm from the scar during epicardial pacing. The HRG volume HRG volume at 0.2-1cm is significantly smaller ($p<0.05$) during endocardial compared to epicardial pacing, significantly larger ($p<0.05$) at 2.5-3.5cm during endocardial compared to epicardial pacing, and similar at 1.5cm. This is illustrated in Figure 3A&C, which shows an example of the spatial distribution of HRG (blue) during endocardial (Figure 3A) and epicardial (Figure 3B) pacing. The difference in HRG volume between endocardial and epicardial pacing is particularly evident when focusing on the highlighted regions within the yellow circles, with a visibly larger reduction in the blue HRG volumes when pacing 3.5cm compared to 0.2cm from the scar for epicardial than for endocardial pacing.

4.2. Transmural APD gradients

Using the patient models, we found that in simulations without a transmural APD gradient (Figure 4), endocardial (Figure 4A) and epicardial (Figure 4B) pacing show similar results with a trend towards reduced HRG volume when pacing away from a scar (Figure 4C), although not significant. Inverting the direction of the APD gradient creates a smaller volume of tissue with HRG when pacing at the endocardial surface (Figure 5A&C) at 3.5cm than at 0.2cm from a scar. This is similar to what is observed for epicardial pacing in the control case (Figure 3B&C), although the difference is not significant (Figure 5C). The HRG volume is significantly larger at

0.2cm during endocardial compared to epicardial pacing and significantly smaller at 3.5cm. Focusing on the highlighted regions indicated by the yellow circles (Figure 5A&B), a slightly smaller HRG volume is observed when pacing 3.5cm compared to 0.2cm from the scar during endocardial (Figure 5A) pacing, whereas the opposite is observed during epicardial (Figure 5B) pacing.

4.3. Fast endocardial conduction

To investigate the impact of the morphological and functional properties of the FEC layer over scar and BZ, we created 6 different setups, including no FEC layer, FEC over healthy and BZ only, and FEC over scar with varying CVs, as shown in the Supplemental Table S1. Epicardial pacing created smaller HRG volumes when pacing away from scar than in proximity to it and endocardial pacing was not sensitive to pacing location relative to scar across all setups (Supplemental Figure S1). Overall, the presence of FEC (setups 2-6) reduced the mean HRG volume at a given pacing location compared to no FEC (setup 1). The level of statistical significance across different setups varied, with setup 6 (FEC over scar with CV 2x the CV of the BZ) showing no significant difference between the HRG volume for epicardial pacing locations and larger variability across models, as evidenced by larger error bars compared to the other setups.

4.4. Idealised models

To demonstrate that these are general findings, independent of the patient specific anatomies, we ran additional simulations using our idealised model. Consistent with the control models, we found that pacing 0.2cm from the scar (Figure 6B) creates a 1.52x larger volume of HRG within 1cm around the scar (yellow circle) during epicardial compared to endocardial pacing (Figure 6A). Conversely, pacing at 3.5cm creates a 0.85x smaller HRG volume during epicardial compared to endocardial pacing. Pacing 3.5cm instead of 0.2cm from the scar creates a substantially smaller HRG volume during epicardial pacing (38% decrease). Conversely, pacing 3.5cm compared to 0.2cm from the scar creates a slightly larger (11%) HRG volume during endocardial pacing. These two findings are also comparable with the patient models, where a significant change in HRG volume is observed during epicardial pacing but not during endocardial pacing.

To further confirm our findings, we ran simulations using the idealised models without a transmural APD gradient and paced at the “endocardium” (Figure 6C) and epicardium” (Figure 6D) surfaces 0.2 and 3.5cm from the scar. The HRG volume in this case is virtually identical for endocardial and epicardial pacing and pacing 0.2cm from the scar creates a larger HRG volume compared to pacing 3.5cm during endocardial (52%) and epicardial (54%) pacing. This differs from the patient models without an APD gradient (Figure 4), where the HRG volume is significantly smaller during endocardial compared to epicardial pacing. This is illustrated in Supplemental Figure S2 and is consistent with a larger volume of viable tissue at the epicardium in the patient models (Supplemental Figure S3), which leads to a larger HRG volume (Supplemental Figures S4) at the epicardium than at the endocardium.

We also investigated the change in repolarization times within the wall in the transmural direction in the absence (Figure 7A&B) and presence (Figure 7C&D) of a transmural APD gradient. In the absence of a transmural APD gradient (Figure 7A&B), the transmural repolarization times increase in the direction of activation for both endocardial and epicardial pacing and with a similar transmural dispersion of repolarization (24.2-27.2ms) for both pacing modalities and locations (0.2 and 3.5cm). In the presence of a transmural APD gradient (Figure 7C&D), the transmural repolarization times also increase in the direction of activation, however, these increase 4.6-5.5x more during epicardial compared to endocardial pacing. Compared to no gradient, the repolarization times increase by ~40% during epicardial pacing and decrease by ~35% during endocardial pacing. Transmural dispersion of repolarization decreases when pacing at 0.2 compared to 3.5cm in all cases, but the difference is small (2.2-3.8ms).

5. Discussion

Our main finding is that endocardial pacing is less arrhythmogenic than epicardial pacing when pacing in proximity to scar. Pacing at the endocardial surface, where APD is longest, provides a mechanistic explanation for this decreased risk during endocardial pacing. The presence and morphological properties of a FEC layer did not substantially affect our findings.

5.1. Mechanisms of decreased VT risk during endocardial pacing

Under physiological conditions, endocardial cells have a longer APD than epicardial cells. This characteristic is responsible for synchronizing repolarization and creating a positive T-wave on ECG[18]. In HF, this transmural APD gradient is reduced compared to healthy conditions[16], but a substantial (~20ms) APD gradient across the wall persists. During epicardial pacing, the physiological direction of repolarization (from epicardium to endocardium) is reversed, increasing transmural dispersion of repolarization and arrhythmia risk[4]. Conversely, the physiological direction of repolarization is preserved during endocardial pacing, suggesting it may be less arrhythmogenic than epicardial pacing.

We investigated the role of the presence and direction of the transmural APD gradient relative to the direction of activation on the HRG volume. Our simulations using idealised computational models predict that propagation from the surface with longest APD to the shortest APD, as is the case during endocardial pacing, attenuates the repolarization gradients due to pacing (Figure 6A). This phenomena can be explained by decreased electronic load of repolarization during endocardial pacing, as epicardial cells repolarize faster than endocardial cells, thus, decreasing (~35%) the total transmural repolarization time (Figure 7B) in comparison with the case without an APD gradient (Figure 7A). Conversely, propagation in the same direction of the APD gradient, as is the case during epicardial pacing, increases the electronic load for repolarization and total transmural repolarization time (~40%), thus, exacerbating the repolarization gradients created due to pacing and creating a larger HRG volume in the vicinity of the scar (Figure 6B).

As the effect of pacing on HRG is attenuated during endocardial pacing due to pacing at the surface with the longest APD, the impact of pacing location relative to scar is decreased and no substantial change in the HRG volume when pacing in proximity and away from scar is observed in the simulations with both idealised (Figure 6A) and patient-specific (Figure 3) models. Conversely, pacing in proximity to instead of away from scar creates larger HRG volumes during epicardial pacing (Figure 3), in agreement with our previous study[5].

The trend towards decreased HRG volume when pacing away from a scar in absence of a transmural APD gradient is similar during endocardial and epicardial pacing in both idealised (Figure 6C&D) and patient-specific (Figure 4C) models.

Although, the HRG volumes during endocardial and epicardial pacing differ significantly in the patient models. This is explained by the fact that there is a larger HRG volume close to the pacing surface than at the opposite surface and that there is a larger volume of viable tissue at the epicardium, due to a larger surface area and less scar. This allows the HRG created by pacing to expand into more tissue during epicardial pacing than during endocardial pacing. See Section 2 of the supplemental material for details. Moreover, the fact that the trend in HRG volume for epicardial and endocardial pacing is reversed when inverting the transmural APD gradient in the patient-specific models (Figure 5) further demonstrates that it is the presence and direction of the transmural APD gradient relative to the direction of propagation that drives the HRG volumes in the vicinity of the scar created during endocardial and epicardial pacing.

5.2. Fast endocardial conduction

Conduction is ~2 times faster at the endocardium than in the remaining myocardium[15] and access to FEC is associated with better resynchronization during endocardial pacing compared to epicardial pacing[3]. A thin layer of tissue is known to survive at the sub-endocardium after infarction[19]. However, to the best of our knowledge, whether FEC is preserved within this thin layer of tissue is currently not known. This surviving sub-endocardium layer is thin (less than 800um[19]), discontinuous, and with fibrosis[20] and fibre disarray[20,21]. Thus, it is unlikely to play a major role in activation and repolarization during endocardial pacing[14].

We investigated the impact of the morphological and functional properties of the FEC layer over scar and BZ. Our simulations predict that the presence of FEC reduces the mean HRG volume compared to no FEC (Supplemental Figure S1). This finding was consistent across all setups, although the level of statistical significance varied. It is worth noting that our sample size is relatively small and the introduction of additional EP heterogeneity may increase variability between models and affect statistical significance.

5.3. Comparison with other studies

Our finding that pacing in opposition to the physiological direction of propagation during epicardial pacing increases transmural dispersion of repolarization (Figure 7) is in agreement with a previous clinical study[4] showing increased transmural

dispersion of repolarization, prolonged QT interval and increased arrhythmia risk during epicardial pacing. However, transmural dispersion of repolarization has been shown to decrease over time in patients who respond to CRT due to reverse remodelling[22]. This is likely to reduce the HRG volume and arrhythmogenic risk due to pacing in responders.

While access to FEC has been shown to improve synchronization during endocardial pacing[1,3], it has not been associated with decreased arrhythmogenic risk. Our results show that the presence of FEC leads to faster activation/repolarization which in turn decreases the HRG volume and relative arrhythmogenic risk (Supplemental Figure S1). Our simulation results show the specific morphological and functional properties of the FEC layer may influence the final HRG volume created during both endocardial and epicardial pacing to a limited extent. However, experimental or clinical evidence on these is currently lacking.

5.4. Clinical implications

The clinical use of endocardium instead of epicardial pacing has increased in the past decades and has shown promising results[2,23]. However, LV endocardial pacing is not without risks. When using a lead to deliver the endocardial stimulus there is increased thromboembolic risk[24] and mitral valve impairment[25], whereas in a leadless system there is the risk of electrode embolization and the need to implant a separate ultrasound transmitter[23]. In addition, all proposed endocardial pacing systems require retrograde arterial access[23] or transseptal puncture[24], which can lead to complications. Moreover, the indications for endocardial pacing are still evolving. Currently, patients are often recruited if they cannot receive or do not respond to conventional CRT[23,24,26,27].

Despite its limitations, endocardial pacing offers a feasible and attractive alternative to conventional epicardial pacing in ICM-HF patients, as it allows pacing at optimal locations for resynchronization[6] while avoiding pacing in proximity to scar and increasing VT risk[5]. Lead guidance[2,6] that indicate that the optimal lead location for epicardial pacing is in the vicinity for scar may also be indications for an endocardial device, given reduced sensitivity to pacing location relative to scar on arrhythmogenic risk during endocardial pacing.

6. Conclusions

Our study showed that endocardial pacing is less arrhythmogenic than epicardial pacing when pacing in proximity to scar in patients with ICM-HF. This behaviour is explained by the presence and direction of transmural APD gradients during HF. The beneficial effect of endocardial pacing on repolarization gradients is slightly enhanced by the presence of FEC.

7. Sources of funding

This research was funded/supported by the National Institute for Health Research (NIHR) Biomedical Research Centre and CRF based at Guy's and St Thomas' NHS Foundation Trust and King's College London. The views expressed are those of the author(s) and not necessarily those of the NHS, the NIHR or the Department of Health. This work was also supported by the Wellcome EPSRC Centre for Medical Engineering at King's College London (WT 203148/Z/16/Z), by the Medical Research Council (MR/N011007/1), and by the British Heart Foundation (RE/08/003, PG/15/91/31812, and PG/16/81/32441).

References

1. Strik M, Rademakers LM, Van Deursen CJM, et al. Endocardial left ventricular pacing improves cardiac resynchronization therapy in chronic asynchronous infarction and heart failure models. *Circ Arrhythmia Electrophysiol*. 2012;5(1):191-200. doi:10.1161/CIRCEP.111.965814

2. Behar JM, Jackson T, Hyde E, et al. Optimized Left Ventricular Endocardial Stimulation Is Superior to Optimized Epicardial Stimulation in Ischemic Patients With Poor Response to Cardiac Resynchronization Therapy: A Combined Magnetic Resonance Imaging, Electroanatomic Contact Mapping, and He. *JACC Clin Electrophysiol*. 2016;2(7):799-809. doi:10.1016/j.jacep.2016.04.006

3. Hyde ER, Behar JM, Claridge S, et al. Beneficial Effect on Cardiac Resynchronization from Left Ventricular Endocardial Pacing Is Mediated by Early Access to High Conduction Velocity Tissue: Electrophysiological Simulation Study. *Circ Arrhythmia Electrophysiol*. 2015;8(5):1164-1172. doi:10.1161/CIRCEP.115.002677

4. Medina-Ravell VA, Lankipalli RS, Yan GX, et al. Effect of epicardial or

biventricular pacing to prolong QT interval and increase transmural dispersion of repolarization: Does resynchronization therapy pose a risk for patients predisposed to long QT or torsade de pointes? *Circulation*. 2003;107(5):740-746. doi:10.1161/01.CIR.0000048126.07819.37

5. Mendonca Costa C, Neic A, Kerfoot E, et al. Pacing in proximity to scar during cardiac resynchronization therapy increases local dispersion of repolarization and susceptibility to ventricular arrhythmogenesis. *Hear Rhythm*. 2019;16(10):1475-1483. doi:10.1016/j.hrthm.2019.03.027

6. Sieniewicz BJ, Behar JM, Gould J, et al. Guidance for Optimal Site Selection of a Leadless LV Endocardial Electrode Improves Acute Hemodynamic Response and Chronic Remodeling. *JACC Clin Electrophysiol*. 2018;4(7). doi:10.1016/j.jacep.2018.03.011

7. Sidhu BS, Lee AWC, Haberland U, Rajani R, Niederer S, Rinaldi CA. Combined computed tomographic perfusion and mechanics with predicted activation pattern can successfully guide implantation of a wireless endocardial pacing system. *EP Eur*. 2019. doi:10.1093/europace/euz227

8. Ukwatta E, Rajchl M, White J, et al. Image-based reconstruction of 3D myocardial infarct geometry for patient specific applications. *Proc SPIE--the Int Soc Opt Eng*. 2015;73(4):94132W. doi:10.1117/12.2082113

9. Bayer JD, Blake RC, Plank G, Trayanova NA. A novel rule-based algorithm for assigning myocardial fiber orientation to computational heart models. *Ann Biomed Eng*. 2012;40(10):2243-2254. doi:10.1007/s10439-012-0593-5

10. Bayer J, Prassl AJ, Pashaei A, et al. Universal ventricular coordinates: A generic framework for describing position within the heart and transferring data. *Med Image Anal*. 2018;45:83-93. doi:10.1016/j.media.2018.01.005

11. Neic A, Campos FO, Prassl AJ, et al. Efficient computation of electrograms and ECGs in human whole heart simulations using a reaction-eikonal model. *J Comput Phys*. 2017;346(346):191-211. doi:10.1016/j.jcp.2017.06.020

12. Ten Tusscher KHWJ, Panfilov A V, Tusscher T. Alternans and spiral breakup in a human ventricular tissue model. *Am J Physiol Hear Circ Physiol*.

2006;291:1088-1100. doi:10.1152/ajpheart.00109.2006

13. Caldwell BJ, Trew ML, Sands GB, Hooks DA, LeGrice IJ, Smaill BH. Three distinct directions of intramural activation reveal nonuniform side-to-side electrical coupling of ventricular myocytes. *Circ Arrhythmia Electrophysiol*. 2009;2(4):433-440. doi:10.1161/CIRCEP.108.830133

14. Mendonca Costa C, Plank G, Rinaldi CA, Niederer SA, Bishop MJ. Modeling the electrophysiological properties of the infarct border zone. *Front Physiol*. 2018;9(APR):356. doi:10.3389/fphys.2018.00356

15. Sano T, Takayama N, Shimamoto T. Directional difference of conduction velocity in the cardiac ventricular syncytium studied by microelectrodes. *Circ Res*. 1959;7(2):262-267. doi:10.1161/01.RES.7.2.262

16. Glukhov A V., Fedorov V V., Lou Q, et al. Transmural dispersion of repolarization in failing and nonfailing human ventricle. *Circ Res*. 2010;106(5):981-991. doi:10.1161/CIRCRESAHA.109.204891

17. Laurita KR, Rosenbaum DS. Interdependence of modulated dispersion and tissue structure in the mechanism of unidirectional block. *Circ Res*. 2000;87(10):922-928. doi:10.1161/01.RES.87.10.922

18. Meijborg VMF, Conrath CE, Opthof T, Belterman CNW, de Bakker JMT, Coronel R. Electrocardiographic T Wave and its Relation With Ventricular Repolarization Along Major Anatomical Axes. *Circ Arrhythmia Electrophysiol*. 2014;7(3):524-531. doi:10.1161/CIRCEP.113.001622

19. Bakker JM, Capelle FJ, Janse MJ, et al. Reentry as a cause of ventricular tachycardia in patients with chronic ischemic heart disease: electrophysiologic and anatomic correlation. *Circulation*. 1988;77(84076). doi:10.1161/01.CIR.77.3.589

20. Spear JF, Horowitz LN, Hodess a B, MacVaugh H, Moore EN. Cellular electrophysiology of human myocardial infarction. 1. Abnormalities of cellular activation. *Circulation*. 1979;59(2):247-256. doi:10.1161/01.CIR.59.2.247

21. Smith JH, Green CR, Peters NS, Rothery S, Severst NJ, Severs NJ. Altered Patterns of Gap Junction Distribution in Ischemic Heart Disease An

Immunohistochemical Study of Human Myocardium Using Laser Scanning Confocal Microscopy. *Am J Pathol*. 1991;139(4). https://www.ncbi.nlm.nih.gov/pmc/articles/PMC1886321/pdf/amjpathol00094-0101.pdf. Accessed March 28, 2017.

22. Itoh M, Yoshida A, Fukuzawa K, et al. Time-dependent effect of cardiac resynchronization therapy on ventricular repolarization and ventricular arrhythmias. *Europace*. 2013;15(12):1798-1804. doi:10.1093/europace/eut145

23. Reddy VY, Miller MA, Neuzil P, et al. Cardiac Resynchronization Therapy With Wireless Left Ventricular Endocardial Pacing. *J Am Coll Cardiol*. 2017;69(17):2119-2129. doi:10.1016/j.jacc.2017.02.059

24. Morgan JM, Biffi M, Gellé L, et al. ALternate Site Cardiac ResYNChronization (ALSYNC): a prospective and multicentre study of left ventricular endocardial pacing for cardiac resynchronization therapy. *Eur Heart J*. 2016;37. doi:10.1093/eurheartj/ehv723

25. Bordachar P, Derval N, Ploux S, et al. Left ventricular endocardial stimulation for severe heart failure. *J Am Coll Cardiol*. 2010;56(10):747-753. doi:10.1016/j.jacc.2010.04.038

26. Rinaldi CA, Auricchio A, Prinzen FW. Left ventricular endocardial pacing for the critically ill. *Intensive Care Med*. 2018;44(6):915-917. doi:10.1007/s00134-018-5062-7

27. Leclercq C, Burri H, Curnis A, et al. Cardiac resynchronization therapy non-responder to responder conversion rate in the more response to cardiac resynchronization therapy with MultiPoint Pacing (MORE-CRT MPP) study: results from Phase I. *Eur Heart J*. 2019. doi:10.1093/eurheartj/ehz109

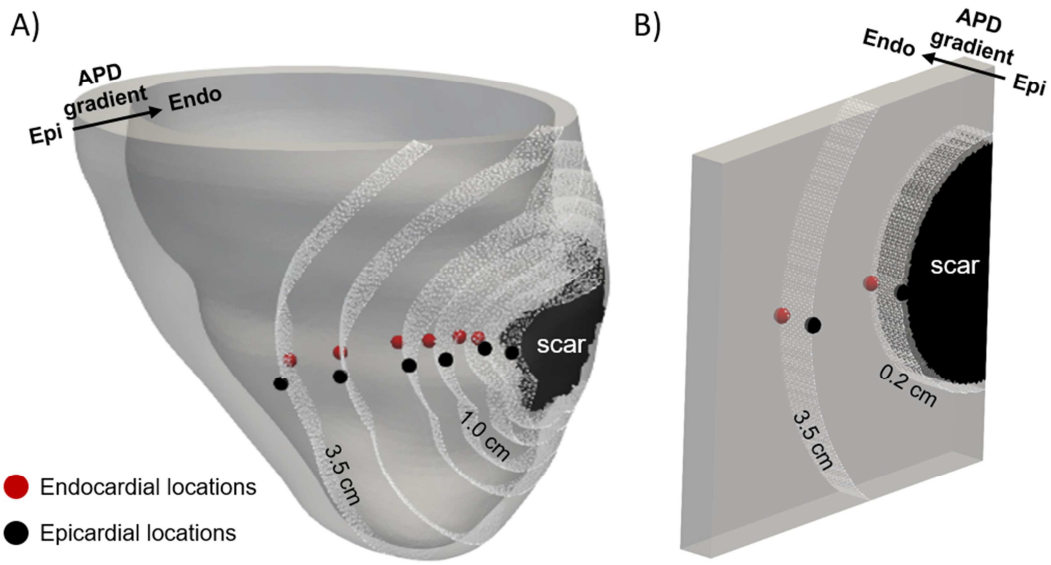

Figure 1: Pacing locations. Endocardial and epicardial pacing locations are shown in red and black, respectively. Distances from the scar surface are indicated by the white point cloud. The epicardial (epi) and endocardial (endo) surfaces and the transmural APD gradient are indicated by the black arrow. A) Patient-specific model: locations were chosen at, from right to left, 0.2, 0.5, 1.5, 2.5, and 3.5cm from the scar surface. B) Idealised model: locations were chosen at 0.2 and 3.5cm from the scar surface.

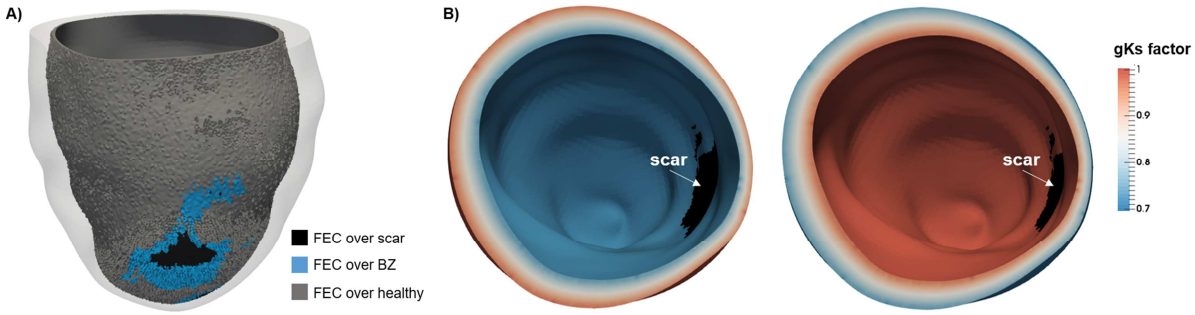

Figure 2: A) Example of a 1mm thick layer of fast endocardial conduction over scar (black), BZ (blue), and healthy tissue (grey). B) Multiplying factor of the slow rectifying postassium current conductance (gKs) across the ventricular wall. Showing an example of the physiological (right) and inverted (left) transmural gradient.

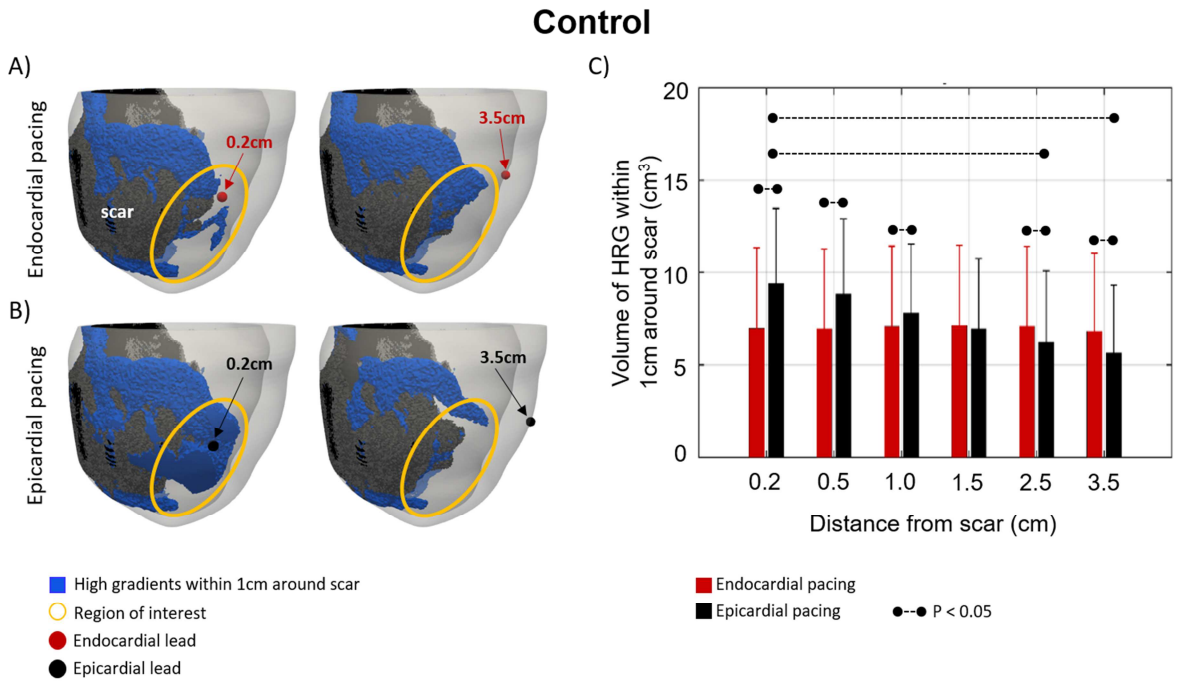

Figure 3: Control case with FEC and a physiological transmural APD gradient. A-B: High repolarization gradients (HRG) within 1cm around the scar (blue) for endocardial (A) and epicardial (B) pacing. Endocardial and epicardial lead locations are shown by red and black filled circles, respectively. Regions of interest are highlighted by yellow circles. C: HRG volume for endocardial (red) and epicardial (black) pacing at 0.2-3.5cm from a scar. Dashed lines indicate a significant (P<0.05) difference.

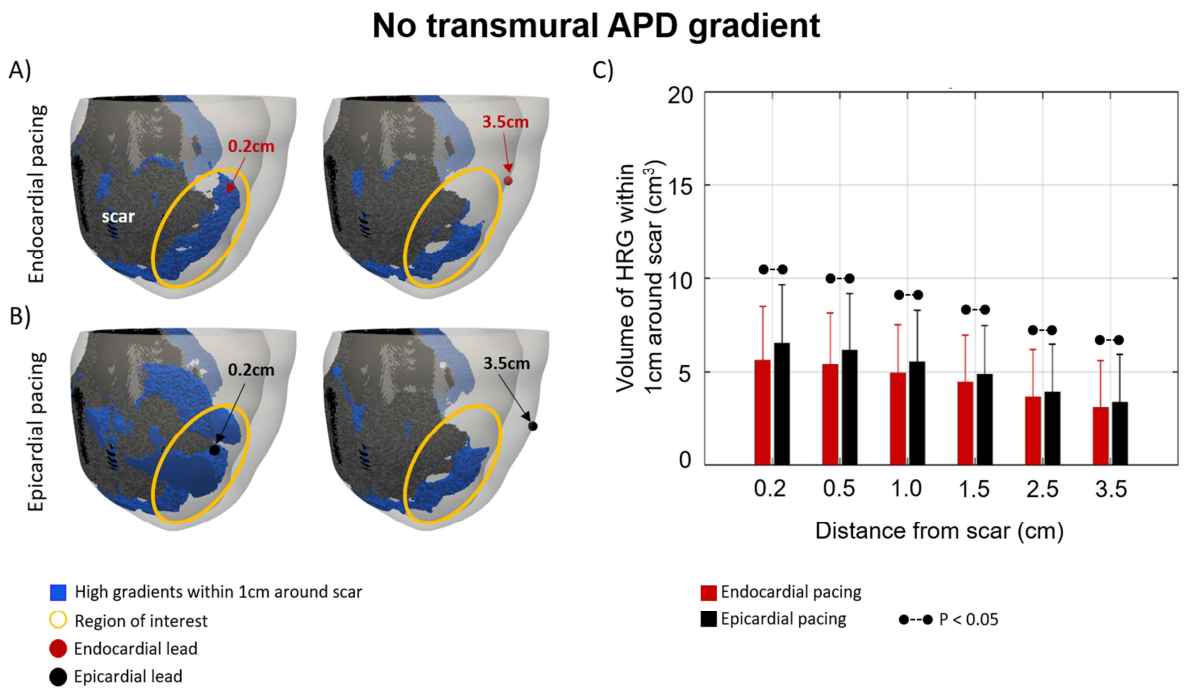

479

480 *Figure 4: No transmural APD gradient case. A-B: High repolarization gradients*
481 *(HRG) within 1cm around the scar (blue) for endocardial (A) and epicardial (B)*
482 *pacing. Endocardial and epicardial lead locations are shown by red and black filled*
483 *circles, respectively. Regions of interest are highlighted by yellow circles. C: HRG*
484 *volume for endocardial (red) and epicardial (black) pacing at 0.2-3.5cm from a scar.*

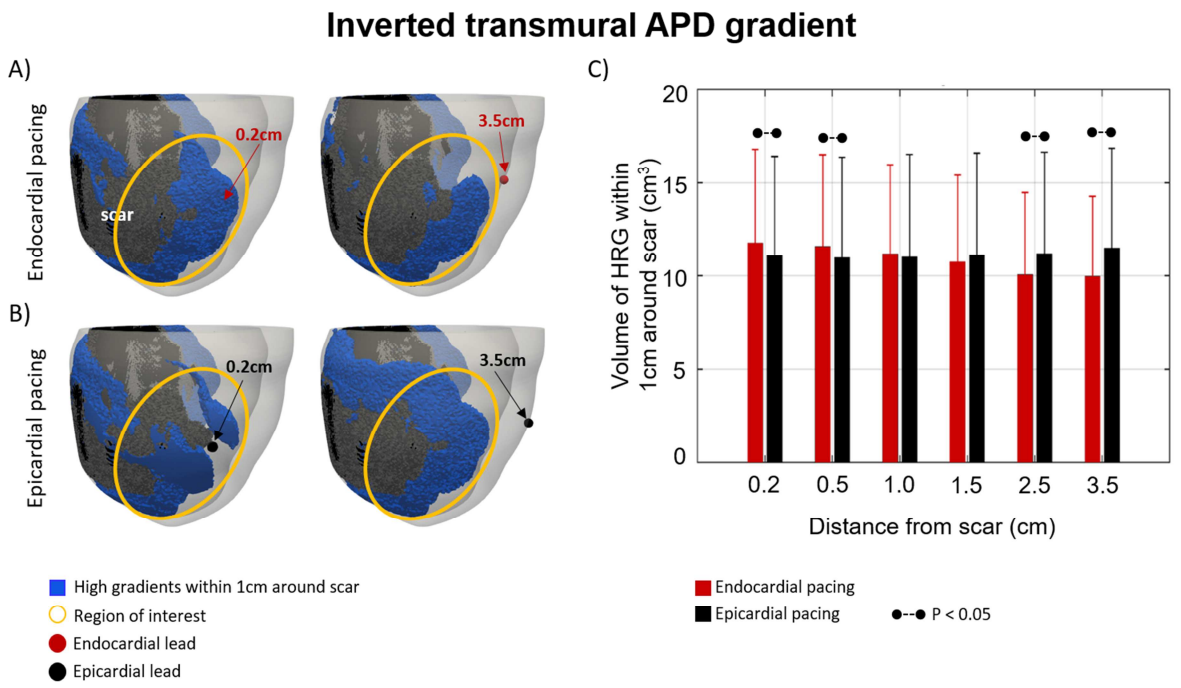

485

486 *Figure 5: Inverted transmural APD gradient case. A-B: High repolarization gradients*
487 *(HRG) within 1cm around the scar (blue) for endocardial (A) and epicardial (B)*
488 *pacing. Endocardial and epicardial lead locations are shown by red and black filled*
489 *circles, respectively. Regions of interest are highlighted by yellow circles. C: HRG*
490 *volume for endocardial (red) and epicardial (black) pacing at 0.2-3.5cm from a scar.*
491 *Dashed lines indicate a significant (P<0.05) difference.*

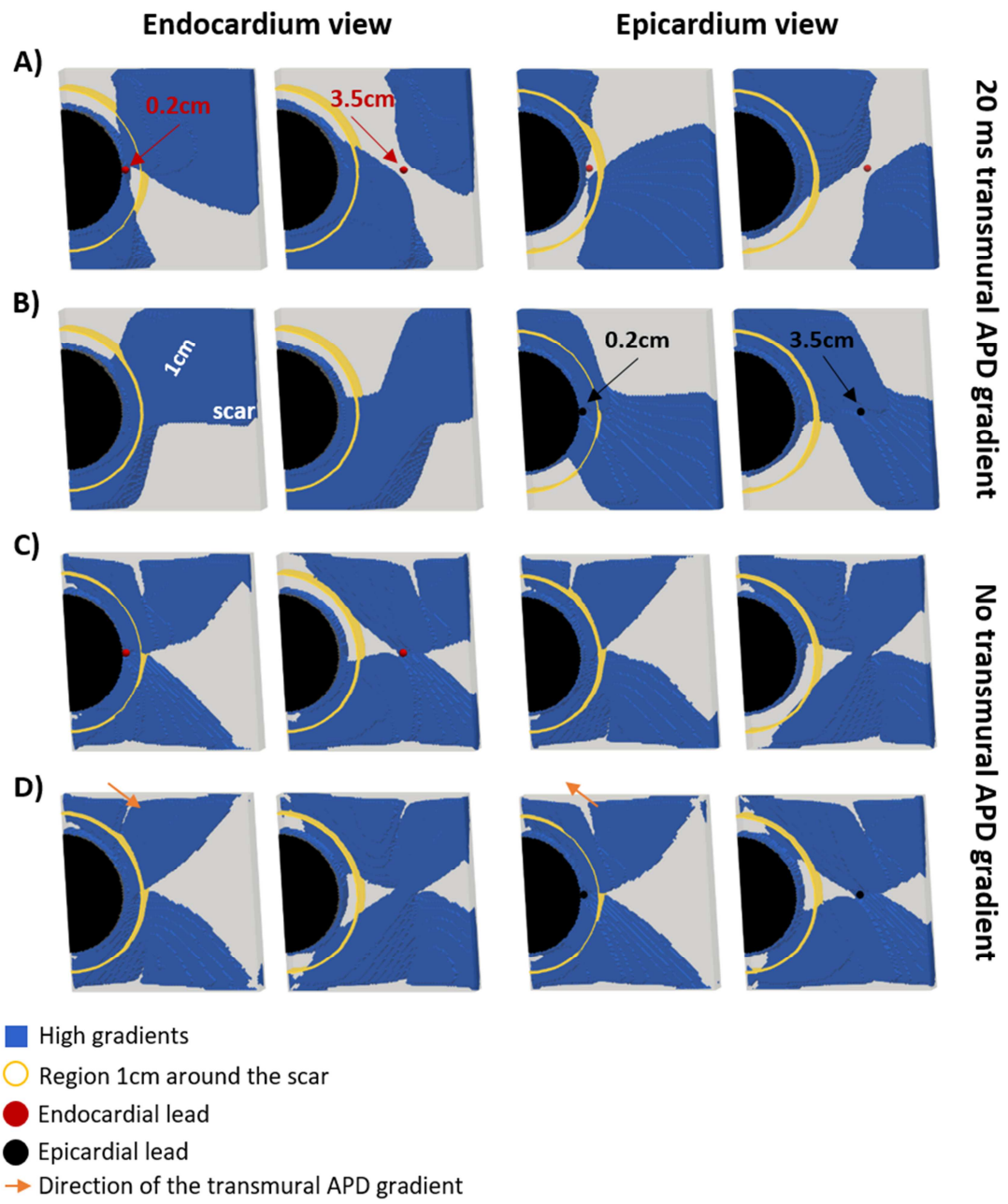

492

493 *Figure 6: Idealised models. High repolarization gradients (blue) for endocardial (A&*
494 *C) and epicardial (B&D) pacing. Showing epicardium and endocardium views when*
495 *pacing 0.2 and 3.5cm from scar. Endocardial and epicardial lead locations are*
496 *shown by red and black spheres, respectively. Region 1cm around the scar is*
497 *highlighted by yellow circles. The orange arrows indicate the direction of the APD*
498 *gradient across the wall.*

499

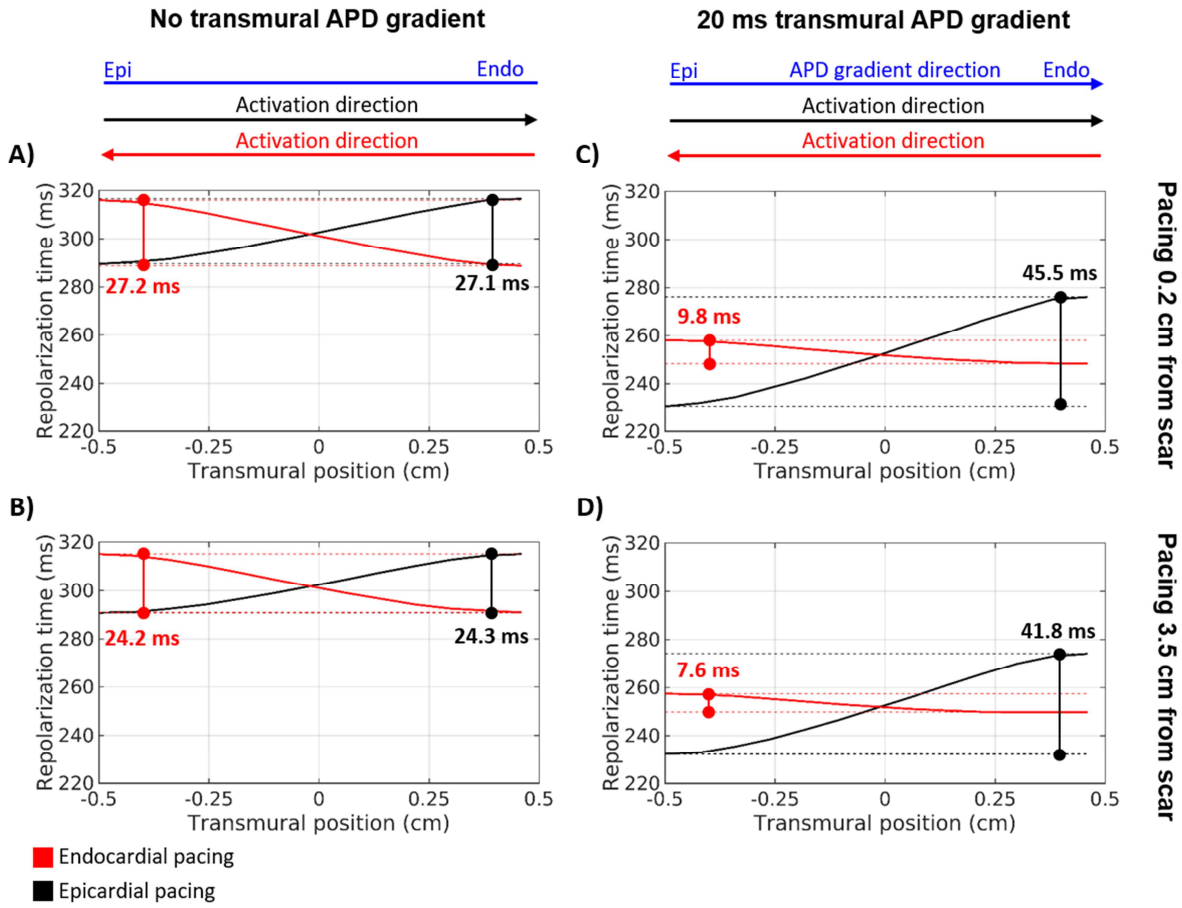

Figure 7: Repolarization times in the transmural direction across the ventricular wall of the idealised models when pacing at the endocardial (red) and epicardial (black) surfaces. Showing results with (C and D) and without (A and B) a transmural APD gradient when pacing 0.2cm (A and C) and 3.5cm (B and D) from the scar. Dashed lines indicate the maximum and minimum repolarization times. The direction of activation during endocardial and epicardial pacing, as well as the direction of the transmural APD gradient (blue) are indicated at the top.